THE JOURNAL OF CHEMICAL PHYSICS VOLUME 44, NUMBER 3 1 FEBRUARY 1966

Temperature and Pressure Dependence of the Elastic Constants of Ammonium Bromide*

C. W. GARLAND AND C. F. YARNELL†

Department of Chemistry, Research Laboratory of Electronics, and *Center for Materials Science and Engineering*
Massachusetts Institute of Technology, Cambridge, Massachusetts

(Received 6 October 1965)

The adiabatic elastic constants of single-crystal ammonium bromide have been measured as functions of temperature and pressure by a pulse-superposition technique. The values at 1 atm and 300°K are: $c_{11}=3.414$, $C'=(c_{11}-c_{12})/2=1.316$, and $c_{44}=0.722$, in units of 10^{11} dyn cm^{-2}. Measurements of c_{11} and C' were not made below the lambda transition at 234.5°K because of a sudden increase in attenuation; c_{44} was not attenuated in this manner and was measured from 105° to 320°K. The elastic constants were measured as functions of pressure between 0 and 12 kbar at constant temperatures which ranged from 255° to 315°K. In this region, which is far from the lambda line, disordered ammonium bromide behaves like a normal CsCl-type crystal.

INTRODUCTION

A LAMBDA transition at 234.5°K in crystalline ammonium bromide was first discovered from heat-capacity measurements.[1] This transition is now established as an order–disorder transition involving the relative orientations of adjacent ammonium ions. However, there are important differences between the ordering process in NH_4Br and that in NH_4Cl, which undergoes a cooperative order–disorder transition at about the same temperature (242.8°K). X-ray,[2] neutron-diffraction,[3] Raman,[4] and infrared[5] investigations show that above their critical temperatures both NH_4Br and NH_4Cl have a CsCl-type cubic structure with the tetrahedral ammonium ions oriented at random with respect to the two equivalent positions in the cubic cell (hydrogen atoms pointing toward nearest-neighbor halide ions). Hettich[6] observed that ammonium bromide does not become piezoelectric below the lambda point but does exhibit double refraction. This result and the low-temperature Raman spectrum led Menzies and Mills[4] to suggest that the ammonium ions in two adjacent unit cells were antiparallel (have opposite orientations relative to the crystallographic axes). Low-temperature x-ray studies[7] have shown that the crystal structure of NH_4Br becomes tetragonal below the transition, and the neutron-diffraction work[3] establishes the location of the hydrogen atoms and confirms that this phase is ordered. The tetragonal unit cell, as shown in Fig. 1, contains two molecules of ammonium bromide.

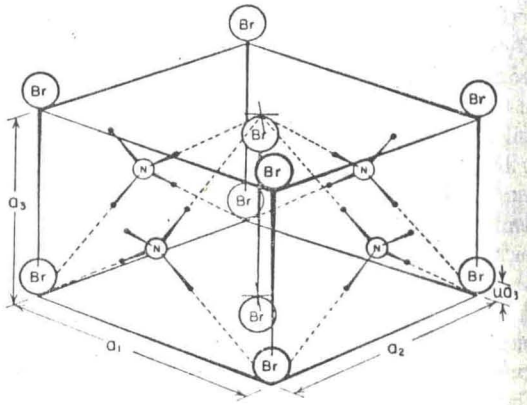

FIG. 1. Unit cell for γ-phase (ordered tetragonal) ammonium bromide. [From E. L. Wagner and D. F. Hornig, J. Chem. Phys. **18**, 305 (1950).]

The ammonium ions are antiparallel ordered in the a_1-a_2 plane and parallel ordered along the a_3 or tetragonal axis. The antiparallel ordering of ammonium ions is stabilized by the bromide ions which are displaced along the tetragonal axis alternately in positive and negative directions with respect to the a_1-a_2 plane by ua_3 where $u=0.02$. The tetragonal distortion is very slight, amounting to an extension of the a_3 axis by only 0.3% relative to the a_1 and a_2 axes.[7] In contrast, the low-temperature ordered phase in ammonium chloride is cubic (CsCl type), and all the ammonium ions are parallel (have same relative orientation with respect to crystallographic axes).

The thermal expansion data also show a marked difference between NH_4Br and NH_4Cl. In NH_4Cl, the lattice undergoes an anomalous contraction[8] when

* This work was supported in part by the Joint Services Electronics Program under Contract DA 36-039-AMC-03200 (E), and in part by the Advanced Research Projects Agency.

† Present address: Bell Telephone Laboratories, Inc., Murray Hill, New Jersey.

[1] F. Simon, C. V. Simson, and M. Ruhemann, Z. Physik. Chem. **129,** 344 (1927); A. G. Cole, Ph.D. thesis, MIT, 1952.

[2] F. Simon and C. V. Simson, Naturwiss. **14,** 880 (1926); G. Bartlett and I. Langmuir, J. Am. Chem. Soc. **43,** 84 (1921).

[3] H. A. Levy and S. W. Peterson, Phys. Rev. **83,** 1270 (1951); **86,** 766 (1952); J. Am. Chem. Soc. **75,** 1536 (1952).

[4] A. C. Menzies and H. R. Mills, Proc. Roy. Soc. (London) **A148,** 407 (1935); R. S. Krishnan, Proc. Indian Acad. Sci. **26A,** 432 (1947); **27A,** 321 (1948).

[5] E. L. Wagner and D. F. Hornig, J. Chem. Phys. **18,** 296 (1950); J. Chem. Phys. **18,** 305 (1950).

[6] A. Hettich and A. Schleede, Z. Physik **50,** 249 (1928); A. Hettich, Z. Physik. Chem. **A168,** 353 (1934).

[7] J. A. A. Ketelaar, Nature **134,** 250 (1934); J. Weigle and H. Saini, Helv. Phys. Acta **9,** 515 (1936); V. Hovi, K. Heiskanen, and M. Varteva, Ann. Acad. Sci. Fenn. Ser. A. VI, No. 144, 1–12 (1964).

[8] Y. Sakamoto, J. Sci. Hiroshima Univ. **A18,** 95 (1954).

ordering occurs on cooling the crystal below the lambda temperature. In NH_4Br the situation is reversed; on cooling there is an anomalous lattice expansion[9] as the bromide crystal undergoes the transition to the ordered tetragonal form. These volume changes associated with changes in ordering make it easy to follow the transition temperatures as a function of applied pressure. Stevenson[10] has obtained the phase diagrams of ammonium chloride, bromide and iodide. His phase diagram for ammonium bromide is reproduced in Fig. 2. (The region encompassed by the sloping lines labeled V_1 to V_{17} in this figure indicates the region of the phase diagram studied in the present investigation.) The β, γ, and δ phases correspond to the structures disordered cubic (CsCl), antiparallel ordered tetragonal and parallel ordered cubic (CsCl), respectively. An α phase corresponding to a disordered NaCl-type cubic structure occurs at high temperatures but is not shown here. There is also a very pronounced hysteresis associated with the γ–δ order–order transition at 1 atm, which is not shown in this figure.

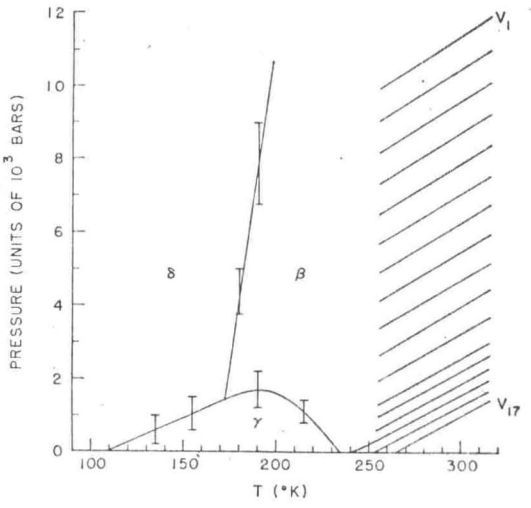

FIG. 2. Phase diagram for NH_4Br. The β phase corresponds to a disordered, CsCl-type cubic phase; the γ phase to an (antiparallel) ordered tetragonal phase; the δ phase to a (parallel) ordered, CsCl-type cubic phase. The vertical bars represent transition points as determined by the static volume measurements of Stevenson (Ref. 10). The set of sloping lines labeled V_1 through V_{17} represent isochores at various volumes.

The present paper reports on a variety of ultrasonic velocity measurements which have been made on single-crystal ammonium bromide. Both longitudinal and transverse waves were studied over a wide range of pressure (0 to 12 kbar) at several constant temperatures in the range 255°–315°K. These data all pertain to the disordered phase away from any transition line, and should provide a clear example of the "normal" behavior of a CsCl-type ammonium halide free from any effects due to ordering. Velocity measurements have also been made as a function of temperature at 1 atm, although data could be obtained below the lambda temperature (234.5°K) only for the transverse wave associated with c_{44}.

This investigation is closely related to previous studies[11,12] of the elastic constants of ammonium chloride as functions of temperature and pressure. These studies show that the shear elastic constants for ammonium chloride (especially c_{44}) varied almost linearly with the volume. Since the volumes of ammonium chloride and bromide vary in an opposite manner at the lambda temperature, we would expect that c_{44} should also vary in an opposite manner. For ammonium chloride, c_{44} increases markedly as the temperature is lowered through the transition; therefore c_{44} for the bromide would be expected to decrease.

The results presented below are given in terms of the variation of the three adiabatic elastic constants c_{11}, c_{44}, C', which can be obtained directly from the experimental sound velocities. Third-order elastic constants are not used, and for pressures above 1 atm the quantities c_{11}, c_{44}, and C' are "effective" elastic constants.[13] The relations between the ultrasonic velocities and the elastic constants of a cubic crystal are well known:

Propagation in the [100] *direction*

$$c_{11}=\rho U_l^2, \tag{1}$$

$$c_{44}=\rho U_t^2, \tag{2}$$

where ρ is the mass density of the crystal, U_l is the velocity of the longitudinal sound wave, and U_t is the velocity of a transverse wave polarized in any direction perpendicular to the [100] axis.

Propagation in the [110] *direction*

$$C'=(c_{11}-c_{12})/2=\rho U_{t'}^2, \tag{3}$$

$$c_{11}+c_{44}-C'=\rho U_{l'}^2, \tag{4}$$

where $U_{l'}$ is the velocity of the longitudinal wave and $U_{t'}$ is the velocity of a transverse wave polarized perpendicular to the [001] axis. Values of $U_{l'}$ were measured only at 1 atm from 250° to 300°K as a check on the internal consistency of the data.

Since the crystal structure of ammonium bromide changes from cubic to tetragonal below the β–γ lambda transition, one must consider the effect of this symmetry change on the elastic constants of a crystalline sample. The tetragonal axis a_3 is now not equivalent to the other axes, and therefore $c_{33}\neq c_{11}$, $c_{13}\neq c_{12}$, and $c_{66}\neq c_{44}$ in the low-temperature phase. Since data were obtained

[9] F. Simon and R. Bergmann, Z. Physik. Chem. **8B**, 255 (1930).
[10] R. Stevenson, J. Chem. Phys. **34**, 1757 (1961).
[11] C. W. Garland and J. S. Jones, J. Chem. Phys. **39**, 2874 (1963).
[12] C. W. Garland and R. Renard, J. Chem. Phys. **44**, 1130 (1966).
[13] R. N. Thurston, J. Acoust. Soc. Am. **37**, 348 (1965).

below T_λ only for transverse waves propagating along a [100] axis in the cubic phase, we shall give the appropriate equations in the tetragonal phase only for that type of wave. When an oriented cubic crystal becomes tetragonal, the transverse velocity U_t is still given by Eq. (2) *if* the tetragonal axis lies parallel to either the direction of wave propagation or the direction of polarization (particle motion). In case the tetragonal axis is oriented perpendicular to *both* the direction of propagation and the direction of polarization, U_t is then given by $\rho U_t^2 = c_{66}$. It is likely that a cubic NH_4Br single crystal is transformed below T_λ into a sample with small tetragonal domains, in which a_3 is oriented parallel to the former x, y, or z axes. If this is so, then the measured ultrasonic velocity will be some kind of mechanical average denoted by $\bar{c}_{44}$.

EXPERIMENTAL WORK

Ultrasonic velocity measurements were made by a McSkimin pulse-superposition method[14,15] at a frequency of 20 Mc/sec. Although this method is experimentally and computationally more difficult than the pulse-echo method, it is capable of very high accuracy since the basic measurement involves a frequency value rather than a time delay and it is possible to evaluate quantitatively the effect of the phase shift γ associated with reflection of the sound wave at the transducer+seal end of the sample. A description of this method and of the necessary electronic apparatus has been given previously[12] and is not included here.

The hydraulic pressure equipment was of conventional design, but since the sample cell was fabricated from 4340 steel it was not considered safe to generate high pressure in it below 250°K. The temperature of this cell could be controlled to within $\pm 0.05°$ by a large thermostat bath. Further details of this pressure equipment and a description of the regulated temperature bath used for measurements at 1 atm are available elsewhere.[12]

The single crystals used in these experiments were grown by a modified Holden process.[16] To obtain a saturated solution at ~45°C, 1200 g of ammonium bromide (analytical reagent grade) and 600 g of urea were added to one liter of distilled water. This large amount of urea was necessary as a habit modifier to prevent dendritic growth and to promote the growth of large cubic crystals with (100) faces. All of the single crystals obtained were pale yellow in color and had some imperfections. Fortunately, these imperfections were either near an edge or near the center of a single face and the transducer could always be located so that they would not lie in the path of the acoustic wave. An analysis of the bromide-ion content indicated that these crystals were at least 99.9% NH_4Br. Three different crystals of ammonium bromide were used to obtain the present data. For Crystals I and II, a pair of natural (100) faces were used without any mechanical cutting or polishing. The lengths (L_{20}) in the [100] direction as measured by a lightwave micrometer at 20°C were 1.0905 ± 0.0005 cm for Crystal I and 1.1935 ± 0.0005 for Crystal II. The third crystal (III) was fly cut to give a pair of parallel (110) faces, and the length L_{20} in the [110] direction was 0.5641 ± 0.0007 cm at 20°C. As a result of handling, exposure to the atmosphere, and seal changes, the path lengths in all these crystals decreased slowly with time. Periodic length measurements were made and corrections were applied to eliminate any small systematic changes in the elastic constants due to path length changes.

A density ρ_{20} of 2.4336 g cm^{-3} was calculated from a lattice constant of 4.0580 Å at 20°C; this unit cell constant is based on several different x-ray investigations around room temperature.[7,17] The elastic constants at 1 atm were obtained as a function of temperature from equations of the type

$$C = \rho U^2 = (L_{20}/L_T)\rho_{20}(2L_{20})^2/\delta^2, \qquad (5)$$

where U is the appropriate velocity, δ is the true round-trip transit time associated with the sound wave, and L_T is the sample length at 1 atm and temperature T. The quantity (L_{20}/L_T) was calculated from the polycrystalline thermal-expansion data of Simon and Bergmann[9] and from the low-temperature x-ray data of Hovi, Heiskanen, and Varteva.[7] Obviously, the x-ray measurements give the tetragonal cell dimensions ($a_3 \neq a_1 = a_2$) below T_λ. On the assumption that a large cubic single crystal is transformed into small domains with the tetragonal axes of these domains lying at random along any one of the original [100] directions, we have taken L_T to be the cube root of the volume below T_λ. The two sets of data are in very good agreement except in the region 230°–235°K, where the x-ray data indicate an almost discontinuous change in L_T with temperature. The rapid but continuous variation obtained from Simon and Bergmann's data was used in this region. However, this choice has a negligible effect (0.05%) on the values of the elastic constants at 1 atm.

To calculate the elastic constants as a function of pressure, it is convenient[18] to introduce another path-length ratio $s(p) = L_1/L_p$, where L_1 is the sample length at a given temperature and 1 atm and L_p is the length at the same temperature under an external applied pressure p. The elastic constants at a given temperature can

[14] H. J. McSkimin, J. Acoust. Soc. Am. **33,** 12 (1961).
[15] H. J. McSkimin and P. Andreatch, J. Acoust. Soc. Am. **34,** 609 (1962); **37,** 864 (1965).
[16] A. N. Holden, Discussions Faraday Soc. **5,** 312 (1949).
[17] V. T. Deshpande and D. B. Sirdesmukh, Acta Cryst. **14,** 353 (1961); V. C. Anselmo and N. O. Smith, J. Phys. Chem. **63,** 1344 (1959).
[18] R. K. Cook, J. Acoust. Soc. Am. **29,** 445 (1957).

then be obtained as a function of pressure from equations of the type

$$C(p)=C(1\text{ atm})\,(\delta_1/\delta_p)^2 s(p), \qquad (6)$$

where δ_1 and δ_p are the transit times corresponding to 1 atm and to a pressure p. In general, the calculation of $s(p)$ requires a knowledge of the isothermal compressibility as a function of pressure. However, an excellent approximation to $s(p)$ can be calculated directly from our present adiabatic velocity data[18] since the difference between the isothermal and adiabatic compressibilities is very small except in the immediate vicinity of the lambda point. [At 300°K and 1 atm, $(\beta^T-\beta^S)/\beta^S$ is only 0.007.] Since $s(p)$ values vary only between 1.00 and 1.02 for the pressure range 0 to 12 kbar, small uncertainties in the $s(p)$ variation do not cause significant errors in the elastic constant values (which depend mostly on δ_1/δ_p).

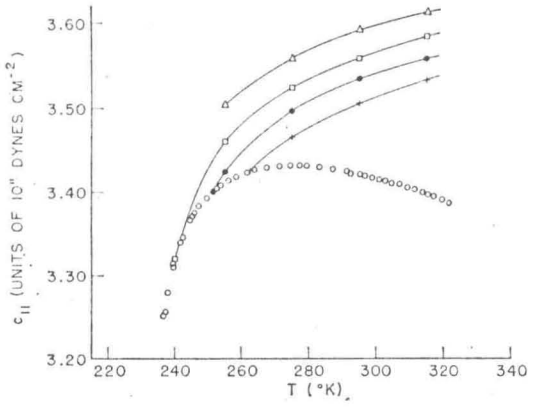

FIG. 3. Variation of c_{11} with temperature. Open circles represent data at 1 atm; for a definition of the symbols used for values at various constant volumes, see the legend of Fig. 5.

For measurements made at 1 atm, the quartz transducers were cemented to the sample with Dow resin 276-V9 as the seal material for all runs between 215° and 320°K. Below 215°K, these seals broke and Nonaq stopcock grease was used in a few runs despite the fact that it seemed to dissolve the sample slowly. Since the Dow resin was soluble in the hydraulic pressure fluid, it was necessary to find a new seal material for the high-pressure work. A polymer of phthalic anhydride and glycerin was found suitable[12] and was used for all the pressure runs.

The Dow resin and Nonaq seals were all very thin. Thus the phase shifts γ were small (between $-5°$ and $-8°$) at all temperatures, and the corrections to the transit times[12] due to phase shifts amounted to only 0.01% at 1 atm. Since all high-pressure measurements were carried out at a frequency equal to the resonance frequency of the transducer at 1 atm, there were appreciable changes in the phase shifts γ as a function of pressure. This effect of pressure on the behavior of the transducers is known[14] and was corrected for. The effect of pressure on the seal is not known and has been neglected.

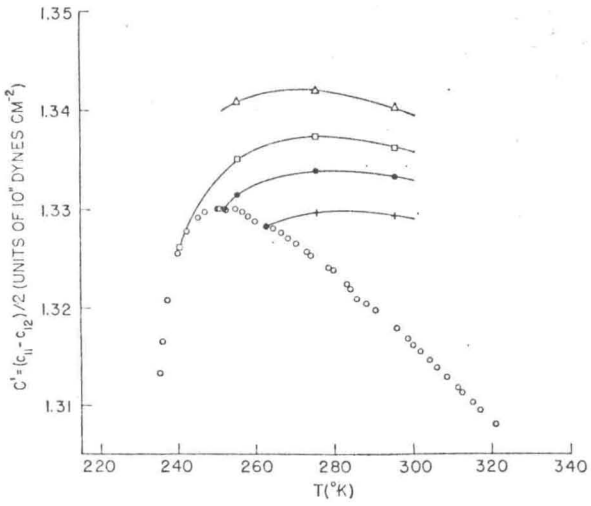

FIG. 4. Variation of C' with temperature. Open circles represent data at 1 atm; for a definition of the symbols used for values at various constant volumes, see the legend of Fig. 5.

RESULTS

Constant-Pressure Data

The open-circle points shown in Figs. 3–5 are experimental data points for the elastic constants c_{11}, c_{44}, and C' as functions of temperature at 1 atm. Smooth-curve values of these directly measured quantities are presented in Table I together with the adiabatic bulk modulus $1/\beta^S$, which can be calculated from

$$1/\beta^S=c_{11}-4C'/3. \qquad (7)$$

Since the temperatures in Table I are all above the lambda point, all entries pertain to the disordered cubic phase of NH_4Br.

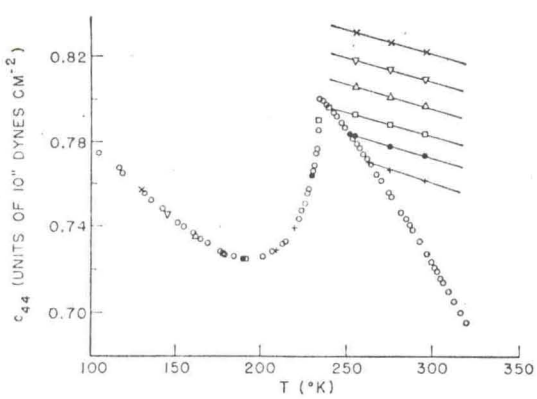

FIG. 5. Variation of c_{44} with temperature. Open circles represent data at 1 atm. Values at various constant volumes are distinguished by the symbols: $X\cdots V_{12}$ ($a_{12}=4.040$ Å); $\nabla\cdots V_{13}$ ($a_{13}=4.0425$ Å); $\triangle\cdots V_{14}$ ($a_{14}=4.045$ Å); $\square\cdots V_{15}$ ($a_{15}=4.0476$ Å); $\bullet\cdots V_{16}$ ($a_{16}=4.0496$ Å); $+\cdots V_{17}$ ($a_{17}=4.0517$ Å).

TABLE I. Smooth-curve values at one atmosphere of the adiabatic elastic constants c_{11}, c_{44}, and C' and calculated values of $1/\beta^S$ for NH_4Br in the cubic disordered phase, all in units of 10^{11} dyn cm^{-2}.

T(°K)	c_{11}	c_{44}	C'	$1/\beta^S$
235	...	0.7992	1.3110	...
236	...	0.7987	1.3171	...
237	3.2640	0.7977	1.3205	1.5033
238	3.2860	0.7968	1.3231	1.5219
240	3.3190	0.7948	1.3260	1.5510
245	3.3694	0.7897	1.3292	1.5971
250	3.3942	0.7842	1.3300	1.6209
260	3.4205	0.7726	1.3289	1.6486
270	3.4293	0.7605	1.3264	1.6608
280	3.4293	0.7478	1.3232	1.6650
290	3.4236	0.7349	1.3197	1.6640
300	3.4144	0.7218	1.3160	1.6597
310	3.4028	0.7083	1.3122	1.6532
320	3.3885	0.6944	1.3083	1.6441

As the temperature was lowered toward the transition temperature, an increase in attenuation was observed. For longitudinal waves in the [100] and [110] direction and for the transverse wave which yields C', the attenuation increased rapidly at the transition temperature and the echoes completely disappeared. As the temperature was lowered below 210°K, echoes slowly began to reappear. The shape of these echoes was very poor, and there was still a great deal of attenuation. Thus it was not possible to make meaningful velocity measurements for c_{11} and C' below the transition.

For the transverse waves associated with c_{44} there was only slight attenuation in the critical region, and data could be obtained over the entire temperature range 100°–320°K including the immediate vicinity of T_λ. Values of c_{44} were determined between 215° and 235°K on all three crystals (using both [100] and [110] propagation directions) and good agreement was obtained. This lends support to the idea that there are small domains with their tetragonal axes randomly oriented along the x, y, or z axes of the original cubic crystal. In that case, the measured ρU_t^2 values below the transition point correspond to an average shear constant $\bar{c}_{44}$ which is related to the single-crystal tetragonal constants by $\bar{c}_{44}=\frac{1}{3}(2c_{44}+c_{66})$. Values of $\rho U_t^2=\bar{c}_{44}$ obtained from measurements along a [100] direction (in the original cubic crystal) are given in Table II and shown in Fig. 4.

TABLE II. Smooth-curve values of the adiabatic quantity $\rho U_t^2=\bar{c}_{44}$ for NH_4Br in the tetragonal (ordered) phase at 1 atm, in units of 10^{11} dyn cm^{-2}.

T(°K)	c_{44}	T(°K)	c_{44}
110	0.7713	205	0.7273
120	0.7639	210	0.7297
130	0.7567	215	0.7331
140	0.7496	220	0.7386
150	0.7427	225	0.7481
160	0.7364	230	0.7627
170	0.7307	231	0.7680
180	0.7265	232	0.7725
190	0.7244	233	~0.778
200	0.7258	234	~0.79

Although it is not shown in Fig. 4, hysteresis was observed in the temperature behavior of c_{44}. On cooling the sample a sharp drop in c_{44} occurred at 234.2°K, whereas the most rapid jump in the c_{44} value on warming the sample occurred at 234.8°K. This temperature hysteresis of 0.6°K is quite comparable to the hysteresis of 0.9°K observed for both c_{44} and C' in ammonium chloride.[12]

The greatest sources of error in these elastic constants at 1 atm are due to uncertainties in the path lengths at 20°C (±0.1%) and ambiguities in the choice of the $n=0$ condition[12] for shear waves (especially for c_{44}). Therefore, to check the possibility that a wrong $n=0$ value had been chosen and also to check the internal consistency of our data, the velocity of the longitudinal wave in the [110] direction was measured as a function of temperature. The experimental value of ρU_l^2 for this wave and that calculated from Eq. (4) using the tabulated values of c_{11}, c_{44}, and C' were within 0.1 percent of each other over the entire temperature range 250°–300°K. This eliminates the possibility of a systematic error in the choice of the $n=0$ value for C'. For c_{44} there is still a possibility that the reported values may be systematically in error by ±0.9%. A propagation-of-errors treatment indicates that the random error in all three elastic constants is about ±0.2% at all temperatures.

TABLE III. The adabatic elastic constants and bulk modulus of ammonium bromide single crystals at room temperature obtained from the present measurements (P) compared with the results obtained by Haussuhl (H) and by Sundara Roa and Balakrishnan (S and B); the bulk modulus of polycrystalline ammonium bromide obtained by Bridgman (B) is included. All values are given in units of 10^{11} dyn cm^{-2}.

Obs.	T(°K)	c_{11}	c_{44}	C'	c_{12}	$1/\beta^S$
P	300	3.414	0.722	1.316	0.782	1.66
H	293	3.38	0.685	1.24	0.91	1.73
S and B	298	2.96	0.53	1.19	0.59	1.38
B	298	...	...	...	...	1.63

The independent adiabatic elastic constants of single-crystal ammonium bromide at room temperature have been measured by Sundara Roa and Balakrishnan[19] and by Haussuhl,[20] who also measured the temperature dependence down to the transition. Table III gives a comparison of the elastic constants and the bulk modulus obtained by these investigators with the results

[19] R. V. G. Sundara Rao and T. S. Balakrishnan, Proc. Ind. Acad. Sci. **28A**, 480 (1948).

[20] S. Haussuhl, Acta Cryst. **13**, 685 (1960).

of the present experiments. Also included is the adiabatic bulk modulus of a polycrystalline sample calculated from Bridgman's isothermal value.[21] The large difference between the present results and those of Sundara Roa and Balakrishnan should not be taken too seriously since the latter were reported to be accurate only to within 10%. The agreement with Haussuhl's elastic constants is not very good, although the slopes of his elastic constants versus temperature agree quite well with those of the present measurements.

Constant-Temperature Data

The experimental values of c_{11}, c_{44}, and C' as functions of pressure at various constant temperatures are shown in Figs. 6–8. Data on the shear constants were obtained with 20-Mc/sec transducers, but these showed a bad tendency to break after several high-pressure runs. Measurements of c_{11} were made at 30 Mc/sec by using a 10-Mc/sec transducer, and this did not break on repeated runs at various temperatures. A tabulation of the smooth-curve values of these elastic constants as a function of pressure is given in Table IV. The limits of error in these elastic constant values at high pressures is somewhat greater than that at 1 atm due to greater uncertainty in the phase-shift correction term. (There is an appreciable increase in γ with an increase in the pressure.)

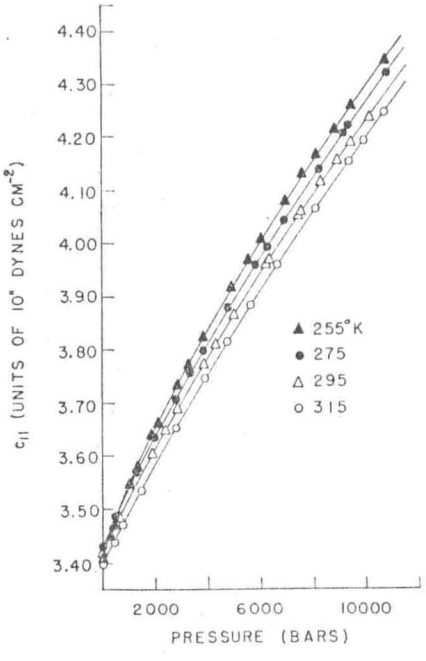

FIG. 6. Dependence of c_{11} on pressure at various temperatures.

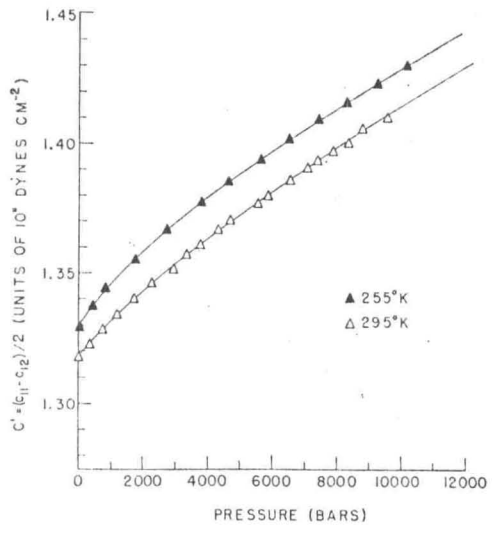

FIG. 7. Dependence of C' on pressure at two temperatures.

Bridgman[21] has measured $\Delta V/V_0$ as a function of pressure for ammonium bromide at 0° and 75°C. A comparison of his values with the values calculated from our present data shows that his values are about 6% high. Bridgman's difference between $\Delta V/V_0$ for a given pressure interval at the two temperatures is about 3 to 4 times greater than that observed in these experiments. The explanation for this difference seems to be that Bridgman's data were taken on a pressed polycrystalline sample, which one would expect to be more

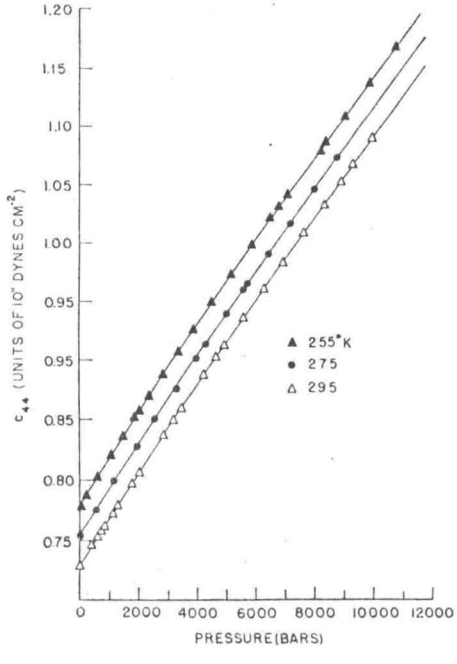

FIG. 8. Dependence of c_{44} on pressure at various temperatures.

[21] P. W. Bridgman, Phys. Rev. **38**, 182 (1931).

TABLE IV. Smooth-curve values of the effective adiabatic elastic constants c_{11}, c_{44}, and C', in units of 10^{11} dyn cm^{-2}, as a function of pressure at various temperatures. Calculated values of $1/\beta^S$ are also given at two temperatures.

$T=315$°K					
p(kbar)	c_{11}	p(kbar)	c_{11}	p(kbar)	c_{11}
0	3.396	4	3.757	8	4.063
2	3.583	6	3.914	10	4.205

$T=295$°K				
p(kbar)	c_{11}	c_{44}	C'	$1/\beta^S$
0	3.419	0.792	1.318	1.662
2	3.615	0.805	1.343	1.824
4	3.789	0.879	1.363	1.972
6	3.949	0.951	1.3815	2.107
8	4.097	1.020	1.398	2.233
10	4.236	1.091	1.4145	2.350

$T=275$°K					
p(kbar)	c_{11}	c_{44}	p(kbar)	c_{11}	c_{44}
0	3.430	0.754	6	3.978	0.975
2	3.639	0.830	8	4.129	1.046
4	3.819	0.903	10	4.272	1.114

$T=255$°K				
p(kbar)	c_{11}	c_{44}	C'	$1/\beta^S$
0	3.411	0.778	1.330	1.638
2	3.654	0.856	1.358	1.843
4	3.843	0.931	1.379	2.004
6	4.010	1.003	1.397	2.147
8	4.162	1.073	1.4135	2.277
10	4.302	1.140	1.4285	2.397

compressible than a single crystal. Indeed, the same kind of discrepancy between single crystal and Bridgman's polycrystalline value is also observed in ammonium chloride.[12]

Constant-Volume Data

In the temperature region above the lambda point, it is possible to combine the results presented above to obtain the variation of the elastic constants with temperature at constant volume. From the known temperature dependence of the cubic cell parameter at 1 atm and the pressure dependence of $s(p)$, one can compute the hydrostatic pressure which must be applied to the crystal at any given temperature in order to maintain its volume at a constant value. This has been done for the 17 different values of the volume: V_1 corresponds to a unit cell dimension of $a_1=3.985$ Å; V_2 through V_{12} correspond to a values which are each 0.005 Å greater than the previous value (up to $a_{12}=4.040$ Å); V_{13} through V_{17} correspond to $a_{13}=4.0425$, $a_{14}=4.045$, $a_{15}=4.0476$, $a_{16}=4.0496$, and $a_{17}=4.0517$ Å. The corresponding p–T isochores are plotted in Fig. 2. With these isochores, one can easily evaluate the effective adiabatic elastic constants at constant volume. Such constants have been plotted in Figs. 3–5 for a few high-volume values as a comparison with the variation at constant pressure. Constant-volume elastic constants are shown in Fig. 9 as a function of temperature for all 17 values of V.

DISCUSSION

Far from the Lambda Transition

As shown in Fig. 2, the principal region of this investigation is the disordered β phase of ammonium bromide. At pressures up to about 3000 bar the elastic constants show a nonlinear variation with pressure due to the fact that the crystal is still in the vicinity of the β–γ lambda line. At higher pressures, farther from the lambda line, the variation is linear as expected for a normal solid having no transition. This is clearly illustrated by the temperature variation of the constant-volume elastic constants shown in Fig. 9. Presented in Table V is a comparison of our data on ammonium bromide with recent data on ammonium chloride[12]; these results are discussed below in the general context of the behavior which is known for alkali halide crystals. The NH_4Cl elastic constants have been measured in a region of the phase diagram which contains the lambda line[12]; therefore the behavior of these constants will be somewhat influenced by the proximity of the order–disorder transition. On the other hand, NH_4Br should be typical of a "normal" CsCl-type crystal (at least above 3000 bar).

Haussuhl[22] has found that all alkali halides of the NaCl type obey the inequality $T'<T_{11}<T_{44}$, where T_{ij} represents $(\partial \ln c_{ij}/\partial T)_p$ at atmospheric pressure and is a negative quantity. For several alkali halides of the CsCl type the inequality has been found[20] to be

$$T_{44}<T_{11}<T'. \tag{8}$$

As shown in Table V, the slopes at 320°K of the elastic constants of ammonium bromide obey this CsCl in-

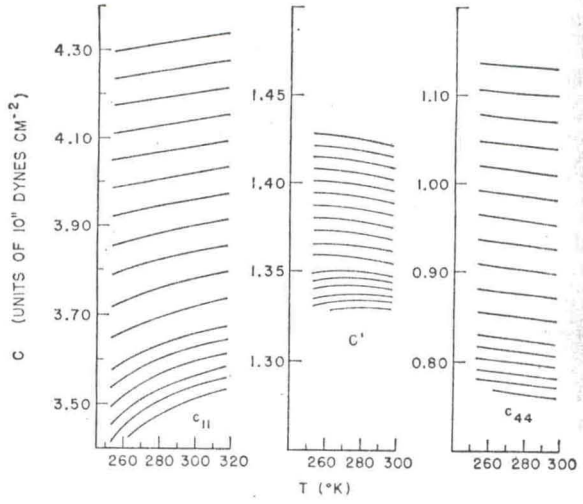

FIG. 9. Adiabatic elastic constants versus temperature at various constant volumes from V_1 to V_{17} (see text). The highest curves correspond to V_1.

[22] S. Haussuhl, Z. Physik **159**, 223 (1960).

TABLE V. The adiabatic elastic constants of ammonium bromide and their temperature and pressure derivatives compared with the results of Garland and Renard (Ref. 12) for ammonium chloride. The value of $\partial \ln c_{11}/\partial T$ at 350°K was measured by Weintraub (Ref. 23); the other $\partial \ln c/\partial T$ values were determined at 320°K. The elastic constants are in units of 10^{11} dyn cm^{-2}; the temperature derivatives are in units of 10^{-4} deg^{-1}, and the pressure derivatives are in units of 10^{-12} cm^2 dyn^{-1}.

	NH_4Cl			NH_4Br		
	c_{11}	C'	c_{44}	c_{11}	C'	c_{44}
c(295°K)	3.814	1.466	0.8753	3.419	1.318	0.7285
$(\partial \ln c/\partial T)_{p=0}$	−1.5 −5.3(350°K)	−2.83	−17.1	−4.32	−2.93	−19.8
$(\partial \ln c/\partial T)_V$	4.0	−0.78	−2.66	3.60	−0.05	−5.86
$(\partial \ln c/\partial p)_{T=295°K}$	4.63	0.81	5.12	3.17	1.03	5.30

equality. At 320°K the slope of c_{11} for ammonium chloride does not seem to fit the pattern; however, if one assumes that c_{11} hasn't reached its limiting "normal" behavior (i.e., that it is still being influenced by the nearby lambda transition), the slopes for the elastic constants would obey the inequality. Indeed, the unpublished results of Weintraub[23] on the variation of c_{11} with temperature between 300° and 375°K indicate that c_{11} becomes linear with respect to T only above 335°K, where $T_{11}=-5.27\times10^{-4}$ deg^{-1}. This value would satisfy the CsCl inequality very well.

The pressure derivatives of the elastic constants, $P_{ij}=(\partial \ln c_{ij}/\partial p)_T$, will obey similar inequalities. Data as a function of pressure are available for several alkali halides of the NaCl type[24] for which the inequality is $P'>P_{11}>P_{44}$. This is reasonable since a decrease in temperature corresponds to an increase in pressure in terms of its effect on the molar volume (and thus the elastic constants). Although no data appear to be available on the pressure dependence of the elastic constants of alkali halides of the CsCl type, the expected inequality would be

$$P_{44}>P_{11}>P'. \qquad (9)$$

Both the ammonium bromide and chloride data obey this inequality over the entire range of temperatures for which pressure measurements have been made; the values of P_{ij} at 295°K, as given in Table V, are typical.

At *constant volume* the inequalities for the temperature derivatives of the alkali halides of the NaCl type which have been studied is $T'<T_{44}<T_{11}$ (constant volume). For the ammonium halides at constant volume the corresponding inequality is

$$T_{44}<T'<T_{11} \qquad \text{(constant volume)}. \qquad (10)$$

This comparison of the behavior of the ammonium halides with that of NaCl-type alkali halides immediately reveals a significant difference: the slope of c_{11} versus temperature at constant volume for ammonium bromide and chloride is *positive* while it is always negative for the NaCl-type salts.[24] This behavior cannot be due to an influence of the lambda transition since for NH_4Br at the lowest volumes (far from the transition) anomalous temperature variations in c_{11} are absent and c_{11} varies linearly with temperature (as a normal crystal should).

Comparison of the elastic constant values in Table V shows that those of ammonium chloride are greater than the corresponding ones for the bromide. This is in general what is observed for all of the alkali halides. As the molar volume (and mass) increases, the stiffness (and thus the elastic constants) decreases. The temperature and pressure derivatives of the elastic constants of ammonium bromide are very similar to those of ammonium chloride, although the pattern is not regular enough to permit scaling. If these derivatives are taken as measures of the anharmonicity of the crystal, then ammonium chloride and ammonium bromide have quite similar anharmonicity.

Near the Lambda Transition

Our information concerning the β–γ transition is limited to data obtained at 1 atm, especially on c_{44} for which measurements could be made below the lambda point.

As the temperature is lowered, c_{44} for ammonium bromide increases linearly with temperature down to the lambda point where it abruptly *decreases* and then at a lower temperature (about 40°K below the lambda point) resumes its normal increase with decreasing temperature (see Fig. 5). The temperature behavior of c_{44} for ammonium bromide is qualitatively compatible with that for ammonium chloride where there is an anomalous increase in c_{44}. This is expected since c_{44} is a sensitive function of the volume, and ammonium chloride contracts on ordering while ammonium bromide expands. A quantitative analysis of the effect of ordering at constant unit-cell dimension is complicated by the

[23] A. Weintraub, senior thesis, MIT, 1963.

[24] D. Lazarus, Phys. Rev. **76**, 545 (1949); R. A. Miller and C. S. Smith, J. Phys. Chem. Solids **25**, 1279 (1964).

tetragonal distortion of the lattice and the displacements of the bromide ions which occur in the γ phase on ordering. Nor is the Ising model theory[25] applied to the NH_4Cl data valid in the case of the β–γ transition in NH_4Br.

The behavior of c_{11} just above the lambda point in ammonium bromide is very similar to that observed in ammonium chloride, whereas the behavior of C' is different in the two cases. Unlike the data for the chloride, C' values for the bromide show a marked anomalous decrease which is apparent as much as 15°K above the lambda point (see Fig. 4). Attenuation of the ultrasonic waves associated with both c_{11} and C' was very high over a considerable range of temperatures below the lambda point. This is presumably due to the presence of domains consisting of tetragonal crystallites with their unique axes lying at random along one of the three original cubic axes. The presence of domains is common in antiferromagnetic crystals and γ-phase ammonium bromide is analogous to an antiferromagnet.

A more extended discussion of the properties of the ordered phase and of the lambda transition region is difficult and inappropriate at this time. New experimental work is now in progress on ammonium bromide in the region 100° to 250°K and 0 to 6 kbar. This will provide information on both the γ and δ phases, as well as new data in the regions of the various transition lines.

[25] R. Renard and C. W. Garland, J. Chem. Phys. **44**, 1125 (1966).

THE JOURNAL OF CHEMICAL PHYSICS VOLUME 44, NUMBER 3 1 FEBRUARY 1966

Order–Disorder Phenomena. I. Instability and Hysteresis in an Ising Model Near Its Critical Point*

CARL W. GARLAND AND RÉMI RENARD†

Department of Chemistry and Center for Materials Science and Engineering, Massachusetts Institute of Technology Cambridge, Massachusetts

(Received 18 August 1965)

The mechanical behavior of a system near a cooperative order–disorder transition point is discussed in terms of an Ising model for a set of spins located on mass particles which form a compressible lattice. With the assumption of weak coupling between the lattice and spin systems, it is shown that this Ising model is unstable in the immediate vicinity of its critical point and undergoes a first-order transition. In addition, many properties should show hysteresis in the critical region. These general conclusions are illustrated by several two-dimensional examples.

INTRODUCTION

IT is a well known but striking fact that substances which undergo cooperative order–disorder transitions usually exhibit anomalous variations in volume which extend over the same temperature range as the lambda spikes in the specific heat. A large amount of theoretical work has been carried out on the thermal properties of such cooperative systems, but little attention has been paid to the mechanical aspects of the problem. Indeed, in most statistical theories the volume of the system is held fixed and it is assumed that experiments could be carried out directly at constant volume. Since it is the pressure rather than the volume which is usually subject to experimental control, the mechanical behavior of a system near a lambda transition point may be of considerable importance.

Our treatment is based on an Ising model for a system of spins located on mass particles which form a compressible lattice. Due to its simplicity, the Ising model is fairly tractable and a great deal has already been done for the fixed-volume case, including an exact solution of the two-dimensional problem by Onsager.[1] In this paper (I), the model is defined and the character of the transition very close to the critical point is investigated. General conclusions about the instability of the system (and a resulting hysteresis) are illustrated by several explicit, two-dimensional examples. In the following paper (II), the model is generalized in terms of stress–strain variables for the two-dimensional case, and the contributions to the elastic constants due to spin ordering is derived in analytic form. Both of these theoretical developments were inspired by recent ultrasonic measurements on ammonium chloride near its lambda transition; and that system, which is analogous to a simple-cubic ferromagnet, provides several excellent confirmations of our predictions. The experimental results on NH_4Cl and their interpretation are given in Paper III.

* This work was supported in part by the Advanced Research Projects Agency.

† Present address: Centre de Recherches, Esso Standard SAF, Mont St. Aignan (Seine Maritime), France.

[1] L. Onsager, Phys. Rev. **65**, 117 (1944).

The possibility of an instability for a compressible lattice near an order–disorder lambda point was first pointed out by Rice,[2] who presented a very general thermodynamic discussion of the problem. A few years later, Domb[3] gave a brief demonstration of the instability of a compressible Ising model, but then the problem appears to have languished for some time. More recently, Bean and Rodbell[4] have demonstrated that magnetic ordering can lead to a first-order transition in the critical region. They based their discussion on the molecular-field theory of ferromagnetism and presented data on MnAs as experimental evidence for their conclusions. Mattis and Schultz[5] have arrived at essentially identical conclusions in their theory of magnetothermomechanics. It is shown here on the basis of a very simple model that an Ising lattice is unstable in the immediate vicinity of its critical point and undergoes a first-order transition with hysteresis. This is proved for a two-dimensional square lattice of ferromagnetic particles in the absence of an external field. Very general conditions are given for observing this effect in a three-dimensional case.

FORMULATION OF THE MODEL

Let us first consider the usual Ising lattice[6] consisting of an array of N fixed sites. Associated with each site are two possible spin orientations—"spin up" and "spin down". For zero external magnetic field, it is customary to write the energy of a given spin configuration as

$$E=-J(q_p-q_a)+\gamma NK/2, \qquad (1)$$

where q_p is the number of nearest-neighbor pairs in the lattice with parallel spins, q_a is the number with antiparallel spins, $\gamma N/2$ is the total number of nearest neighbors ($\gamma=4$ for two-dimensional square lattice, $\gamma=6$ for three-dimensional sc lattice, etc.), and J and K are defined by

$$J=(U_a-U_p)/2; \qquad K=(U_a+U_p)/2. \qquad (2)$$

In the above, U_p is the potential energy due to spin interaction between a nearest-neighbor pair of parallel spins and U_a is the interaction energy for a pair of antiparallel spins. The case $J>0$ corresponds to ferromagnetism. For simplicity, the model is given only for the case of isotropic spin interactions. Thus, the spin partition function is $Q_s=Q_I(0, H)\exp(-\gamma NK/2kT)$, where $Q_I(0, H)$ is the well-known Ising partition function at zero field as a function of $H\equiv J/kT$.

Instead of being concerned with the thermal behavior of a "clamped" system of spins only, we wish to consider the mechanical behavior of a more realistic model in which the localized spins are associated with mass particles (atoms, ions or molecules) which form a compressible lattice. Indeed, an "unclamped" array of spins only is usually unstable and it is the interaction between mass particles which stabilizes the composite system. We *assume* weak coupling between the lattice and spin systems; i.e., we assume that $Q=Q_sQ_l$, where Q_l is the partition function of the particle lattice. This is the crucial feature of our model. Almost all theories of order–disorder phenomena are based on the implicit hypothesis that a configurational partition function can be written without taking into account strong coupling between the spins and the rest of the system.[7] It is possible to check on this weak-coupling assumption for regions far away from the critical point since many properties (e.g., heat capacity, thermal expansion, elastic constants) then depend essentially on the lattice contribution. If the coupling is weak, these properties should have comparable temperature and pressure dependences in the completely ordered and completely disordered state, assuming that these two states belong to the same crystallographic group. It is, however, possible to imagine that the coupling will be strong *only* in the critical region. Since there is no theoretical evidence that this must be true in general, we have made the simpler assumption and present below the consequences of weak coupling in an Ising model.

It proves convenient to rewrite the over-all partition function of the system in a new form

$$Q=Q_sQ_l=Q_I\exp(-\gamma NK/2kT)Q_l=Q_IQ_{dl}, \qquad (3)$$

where Q_{dl}, the partition function for the *disordered lattice*, includes both the usual lattice contribution of a normal crystal and the interactions between randomly-oriented spins. As a result of Eq. (3) all the thermodynamic functions can be written as a sum of two independent contributions; in particular for the Helmholtz free energy, $A=A_I+A_{dl}=-kT\ln Q_I-kT\ln Q_{dl}$. The contribution to the properties of the system which arise from the Q_{dl} term can be deduced empirically from experiments performed on crystals considerably above their lambda points. We emphasize here the contribution to various properties due to the Q_I term which describes the spin ordering. The expressions for the configurational internal energy and specific heat at constant volume are well known[6] and can be written as

$$U_I=-Jd\ln Q_I/dH, \qquad (4)$$

$$C_I=kH^2d^2\ln Q_I/dH^2, \qquad (5)$$

since Q_I is a function only of $H\equiv J/kT$ and J is not a function of temperature. The quantity J will, however, be a function of the spacing between lattice sites.

[2] O. K. Rice, J. Chem. Phys. **22,** 1535 (1954).
[3] C. Domb, J. Chem. Phys. **25,** 783 (1956).
[4] C. P. Bean and R. S. Rodbell, Phys. Rev. **126,** 104 (1962).
[5] D. C. Mattis and T. D. Schultz, Phys. Rev. **129,** 175 (1963).
[6] K. Huang, *Statistical Mechanics* (John Wiley & Sons, Inc. New York, 1963), Chaps. 16 and 17; H. S. Greene and C. A. Hurst, *Order–Disorder Phenomena* (Interscience Publishers, Inc., New York, 1964), Chaps. 2, 3, and 6.

[7] Some work has been done on the coupling between ordering and vibrational motions for a one-dimensional binary alloy; A. A. Maradudin, E. W. Montroll, and G. H. Weiss, Solid State Phys. Suppl. 3., pp. 188–212 (1963).

Thus, we can define a *spin* (or Ising) *pressure* by $p_I=-(\partial A_I/\partial V)_T$; this contribution to the total pressure is directly related to the Ising energy U_I by

$$p_I=kT\left(\frac{\partial \ln Q_I}{\partial J}\right)_T\frac{dJ}{dV}=\left(\frac{d\ln Q_I}{dH}\right)\frac{dJ}{dV}=-\frac{U_I}{NJ}\frac{dJ}{dv}, \quad (6)$$

where $v=V/N$ is the volume per lattice site. Note that U_I has a negative value in the ordered phase and goes to zero as the spins disorder.

INSTABILITY AND HYSTERESIS

At a given temperature T a system is stable, at least locally, if the Helmholtz free energy satisfies the condition $(\partial^2 A/\partial V^2)_T\geq 0$. For the model considered above, this stability condition requires that

$$-(\partial p_{dl}/\partial v)_T-(\partial p_I/\partial v)_T\geq 0, \quad (7)$$

where $(\partial p_I/\partial v)_T$ is found from Eq. (6) to be

$$(\partial p_I/\partial v)_T=(T/NJ^2)C_I(dJ/dv)^2-(U_I/NJ)(d^2J/dv^2). \quad (8)$$

Since $(\partial p_{dl}/\partial v)_T$ is related to $\beta_{dl}{}^T$, the isothermal compressibility of the disordered lattice, by

$$1/\beta_{dl}{}^T=-v(\partial p_{dl}/\partial v)_T \quad (9)$$

one can write the stability condition as

$$\frac{1}{\beta_{dl}{}^T}-\frac{vT}{NJ^2}C_I\left(\frac{dJ}{dv}\right)^2-\frac{vU_I}{NJ}\left(\frac{d^2J}{dv^2}\right)\geq 0. \quad (10)$$

Now $1/\beta_{dl}{}^T$ will in general have a finite positive value which is a slowly varying function of temperature, while J and its derivatives with respect to v will be finite non-zero quantities which are independent of temperature. The Ising internal energy will also be finite at all temperatures; but the configurational heat capacity at constant volume, C_I, is known to approach very large values in the vicinity of the critical point. The behavior of C_I is the crucial factor. If C_I approaches $+\infty$ at the critical temperature, there must be an instability near that point unless the particle lattice is completely incompressible (in which case, $1/\beta_{dl}{}^T=+\infty$). This result depends only on our assumption of weak coupling in the model.

For the two-dimensional Ising model an exact analytical expression for Q_I (and thus C_I) is available,[1] and C_I is known to have a logarithmic singularity at T_c. Equations (6)–(10) are still valid in two dimensions if v is replaced by σ, the surface area per lattice site, and p is understood to be a surface pressure defined by $-[\partial A/\partial(N\sigma)]_T$. In this case, the instability of a compressible lattice in the immediate vicinity of its critical point follows directly from Eq. (10). This instability will cause the system to undergo a spontaneous first-order phase transition across the unstable region. Associated with this first-order transition is the possibility of hysteresis. To *illustrate* these conclusions we discuss below several different aspects of the behavior of a two-dimensional model. In this case, Eq. (6) allows us to easily calculate the Ising pressure p_I from the known expression[1] for U_I if J and $dJ/d\sigma$ are specified. For a ferromagnet, J is simply related to the critical temperature ($J=0.44069\ kT_c$) and it is physically reasonable to expect that $dJ/d\sigma<0$. Let us represent J by the form α/σ^n, (where n is a small integer) as an illustrative example. A typical disordered-lattice pressure will be represented over a small range of σ by

$$p_{dl}=a_0+a_1T-b\sigma, \quad (11)$$

where a_0, a_1, and b are positive constants.

Constant External Pressure

For a system at equilibrium under an external applied pressure, it is necessary that $p_{\text{ext}}=p_{dl}+p_I$. We treat the simplest case of zero external pressure, for which $p_I=-p_{dl}$. Figure 1 shows a plot of p_I and $-p_{dl}$ against σ at several temperatures $T_1<T_2<\cdots T_6<T_7$. An intersection of the two appropriate isotherms will give the equilibrium area σ under zero external pressure if the stability condition (7) is satisfied (that is, if the slope of $-p_{dl}$ is *greater* than that of p_I). Now consider the change in σ with T for $p_{\text{ext}}=0$. As the temperature increases from T_1 to T_5, σ can increase continuously from σ_1 to σ_5 (Points 1 to 5 on Fig. 1), but as $T\rightarrow T_5$ from *below* the system becomes unstable ($\partial^2 A/\partial\sigma^2=0$) at Point 5 and there must be a first-order change in area from σ_5 to σ_5'. On further heating, σ increases continuously from σ_5' to σ_7. However, on cooling from T_7 to T_3 the area can decrease smoothly from σ_7 to σ_3'. As $T\rightarrow T_3$ from *above* the instability occurs at Point 3′ and there is a first-order change from σ_3' to σ_3. Below T_3, σ decreases smoothly on cooling. Thus, there can be a hysteresis loop near the critical point with a first-order jump in σ at T_5 on heating and a first-order drop in σ at T_3 on cooling; this is shown schematically in an inset on Fig. 1. The values T_3 and T_5 determine the maximum width of this loop since the system becomes *mechanically* unstable at Points 5 and 3′. Actually, there is a temperature T_4 for which the free energy at Point 4 equals that at Point 4′; complete thermodynamic equilibrium would give a first-order transition at T_4 and no hysteresis. The region between 4 and 5 on heating or 4′ and 3′ on cooling is only metastable. It is easy to show that a Maxwell equal-area rule is valid for determining T_4 in this system.

The lower inset on Fig. 1 presents a *schematic* sketch of the temperature dependence of $1/\beta^T$ in the critical region. On warming, as T_5 is approached from *below*, $1/\beta^T$ approaches zero and then jumps to the value B after the first-order transition occurs. On cooling, as T_3 is approached from *above*, $1/\beta^T$ vanishes and jumps to the value A after the transition. If the system is in complete thermodynamic equilibrium, $1/\beta^T$ never van-

FIG. 1. Ising mod
at vanishi
of *curves*
evenly-spa
T_7. The f
drawn to
with typi
expansion
bers 1 an
isotherms
sent sche
pendence
rocal isot

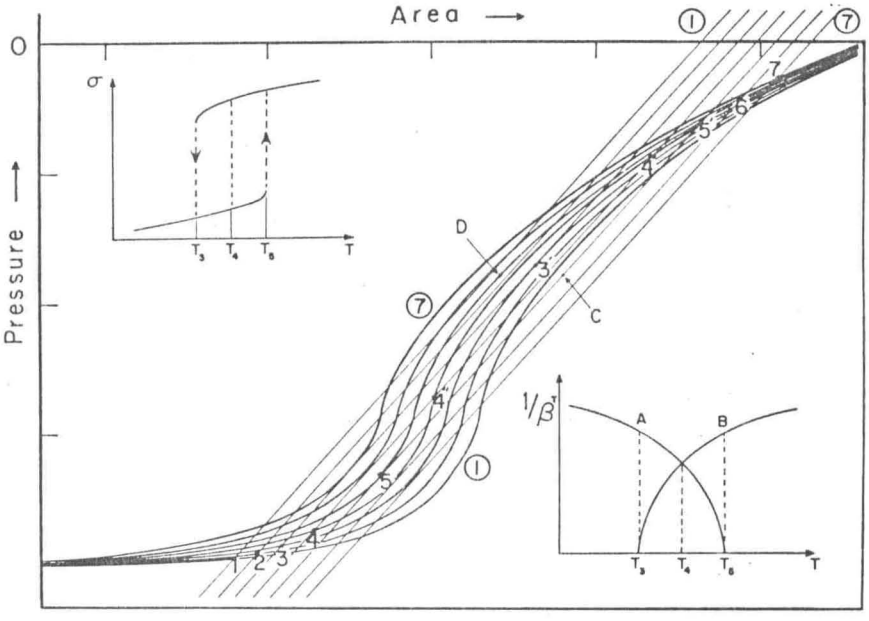

FIG. 1. Behavior of a two-dimensional Ising model as a function of temperature at vanishing external pressure. The family of *curves* p_I were calculated at seven evenly-spaced temperatures from T_1 to T_7. The family of *straight lines*—p_{dl} were drawn to represent a disordered lattice with typical compressibility and thermal expansion coefficients. The encircled numbers 1 and 7 indicate the spin and lattice isotherms at T_1 and T_7. The insets represent schematically the temperature dependences of the area σ and of the reciprocal isothermal compressibility $1/\beta^T$.

ishes but has a singular point at T_4. If the transition occurs in the metastable region but before the mechanical instability point is reached, $1/\beta^T$ will show hysteresis and discontinuities but does not vanish.

If an actual crystal behaves like this model, it is impossible to bring it arbitrarily close to a lambda point: a first-order transition occurs before the temperature reaches the theoretical critical temperature. Indeed, unless great care is taken to achieve true thermodynamic equilibrium, there are a range of temperatures (such as T_3 to T_5 in Fig. 1), where the properties depend on the history of the sample.

Constant Temperature

Let us look at the variation of area σ as a function of the applied pressure p_{ext}. Figure 2 shows, at a given temperature, the Ising pressure and the negative of the disordered-lattice pressure as functions of σ. At zero external pressure, the equilibrium point is at A, which corresponds to a largely disordered system. As the external pressure is increased, the ordering of the system increases and the area σ decreases smoothly until the pressure reaches a value equal to BB' at which mechanical instability occurs. The system spontaneously contracts to an area σ_C corresponding to Point C, which is the new equilibrium state under this external pressure of magnitude $p_3=CC'=BB'$. A further increase in the external pressure causes a smooth decrease of the area and completes the ordering. If the pressure is now reduced, the system is mechanically stable until the area reaches the value $\sigma_D>\sigma_C$. At D the system is mechanically unstable and spontaneously expands to the value σ_E, the new equilibrium area under this pressure of magnitude $p_1=EE'=DD'$. Again the possibility of hysteresis is predicted in a region which corresponds to metastable (or local) equilibrium. If the system were in complete thermodynamic equilibrium a first-order transition without hysteresis would take place at pressure p_2.

Constant Area

If the area is maintained constant by an applied pressure and not by rigid clamping, Inequality (10) is still valid. Therefore on each curve $p_I(T)$ for a given area, there is a forbidden zone in which the intersection of the isochores $-p_{dl}(T)$ and $p_I(T)$ does not correspond to a stable state. On Fig. 3 are plotted several Ising isochores corresponding to areas $\sigma_1<\sigma_2<\cdots\sigma_6<\sigma_7$. The

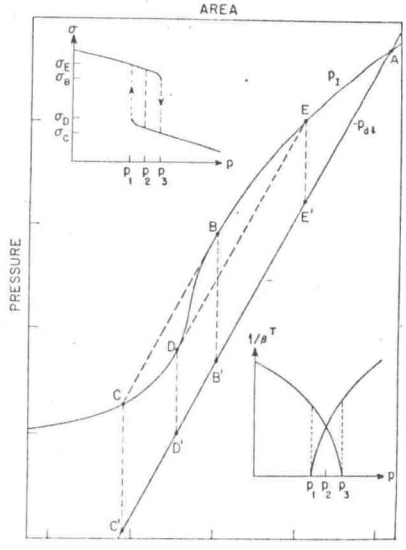

FIG. 2. Behavior of a two-dimensional Ising model as a function of pressure at constant temperature. The insets represent schematically the pressure dependence of the area σ and of the reciprocal isothermal compressibility $1/\beta^T$.

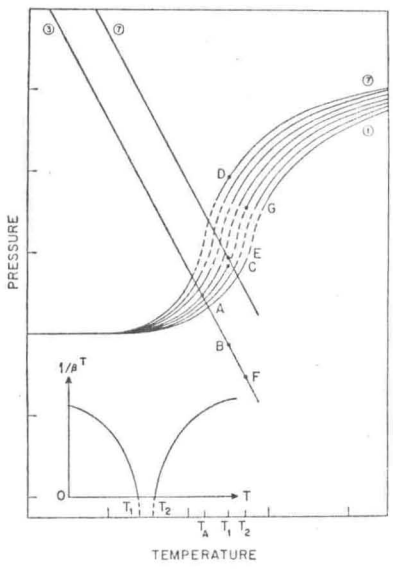

FIG. 3. Behavior of a two-dimensional Ising model at constant volume. The family of *curves* p_I were calculated at seven evenly spaced areas from σ_1 to σ_7. The *lines*—p_{dl} were drawn to represent a disordered lattice with typical compressibility and thermal expansion coefficients. The encircled numbers indicate the spin and lattice isochores at the given areas. The inset represents schematically the temperature dependence of the reciprocal isothermal compressibility $1/\beta^T$.

forbidden zones are shown as dashed lines. The negative disordered-lattice isochores $-p_{dl}(T)$ are also plotted for areas σ_3 and σ_7. Let us assume we want to keep the system at a constant area σ_3. Under zero external pressure, the equilibrium point is at A, corresponding to a temperature T_A. As the temperature is increased, the system can be kept at constant area σ_3 by applying an external pressure. When the temperature reaches T_1 where the appropriate external pressure is of magnitude $p_1=BC$, the system becomes mechanically unstable. Then the area will spontaneously *increase* to (say) σ_7 which is a stable state at temperature T_1 under an external pressure $p_1=BC=DE$. In the range $T_1<T<T_2$ it is impossible, by any manipulation of the external pressure,[8] to keep the area at value σ_3. Above T_2 it is again possible to maintain the area σ_3. If the metastable equilibrium is disrupted before the mechanical instability point is reached, the range of temperature over which it is impossible to maintain constant area is widened somewhat.

An inset on Fig. 3 shows the schematic variation of $1/\beta^T$ as a function of temperature for a constant area σ_3. At T_1 and T_2, $1/\beta^T$ vanishes; the dashed lines represent the behavior expected if the area could be kept constant (i.e., if one could work in an unstable region). Because of the instability, the area of the crystal between T_1 and T_2 depends on the way the experimental run is conducted. The actual area can correspond to an equilibrium point close to or far from an instability point. As a result, experimental values for $1/\beta^T$ between T_1 and T_2 can vary between 0 and an upper value corresponding to the completely disordered state. Consequently, compressibility measurements at constant area σ_3 are meaningful only outside the temperature interval $T_1<T<T_2$.

CONCLUSION

The preceding illustrations of instability and hysteresis near a critical point have been given in terms of a two-dimensional model. The generalization of the discussion to a three-dimensional Ising model is quite easy. For a real three-dimensional crystal, $1/\beta_{dl}{}^T$ is experimentally known to be finite at temperatures above T_c, and according to our model it is therefore finite at all temperatures. Recent approximate calculations[9,10] indicate that C_I for a cubic Ising model does approach infinity as T approaches T_c. If so, there will be a range of temperatures in the critical region for which the inequality (10) cannot be satisfied. If C_I does not in fact become infinite at T_c the system may display a lambda transition. However, a very large finite value for C_I can still cause a soft crystal (for which $1/\beta_{dl}{}^T$ is small) to become unstable. If the crystal does become unstable before the critical point is reached, there is also a region of metastability and the strong probability of hysteresis. The general nature of the hysteresis is the same as that shown in Figs. 1–3 since the isotherms and isochores for p_I and p_{dl} have qualitatively the same shape in three dimensions as in two (although the p_I curve is less symmetrical in three dimensions).

In summary, a first-order transition is to be expected in crystals near a lambda point unless some special kind of strong lattice–spin coupling is invoked. The observable effects of this instability should be large only when (a) the lattice is quite compressible ($\beta_{dl}{}^T$ large) and (b) the spin interactions are a sensitive function of distance (dJ/dv large). Thus, this phenomenon is difficult to observe in many ferromagnetic solids. In Paper III we hope to show for ammonium chloride, which satisfies both Conditions (a) and (b), that the experimental data conform very well to the predictions of this model.

[8] There is, in principle, a way to keep the volume of a three-dimensional crystal constant. It consists of clamping the crystal in an infinitely rigid holder. This is equivalent to making the disordered lattice incompressible. In this case inequality (10) is fulfilled at any temperature. In practice this can not easily be realized; one usually places the sample in a fluid under pressure which is externally set at some given value.

[9] J. W. Essam and M. E. Fisher, J. Chem. Phys. **38**, 802 (1963).

[10] D. S. Gaunt, M. E. Fisher, M. F. Sykes, and J. W. Essam, Phys. Rev. Letters **24**, 713 (1964).